Journal of Controlled Release 160 (2012) 666–675

Contents lists available at SciVerse ScienceDirect

Journal of Controlled Release

journal homepage: www.elsevier.com/locate/jconrel

# Enhanced neurotrophin-3 bioactivity and release from a nanoparticle-loaded composite hydrogel

Jason C. Stanwick [a], M. Douglas Baumann [a,b], Molly S. Shoichet [a,b,c,*]

[a] Department of Chemical Engineering and Applied Chemistry, University of Toronto, 200 College Street, Toronto, ON, Canada M5S 3E5
[b] Institute of Biomaterials and Biomedical Engineering, 164 College Street, Room 407, Toronto, ON, Canada M5S 3G9
[c] Department of Chemistry, University of Toronto, 80 St. George Street, Toronto, ON, Canada M5S 3H6

ARTICLE INFO

*Article history:*
Received 5 January 2012
Accepted 26 March 2012
Available online 4 April 2012

*Keywords:*
Neurotrophin-3
Poly(lactic-co-glycolic acid) (PLGA)
Nanoparticle
Hydrogel
Spinal cord injury
Drug delivery

ABSTRACT

Neurotrophin-3 (NT-3) has shown promise in regenerative strategies after spinal cord injury; however, sustained local delivery is difficult to achieve by conventional methods. Controlled release from poly(lactic-co-glycolic acid) (PLGA) nanoparticles has been studied for numerous proteins, yet achieving sustained release of bioactive proteins remains a challenge. To address these issues, we designed a composite drug delivery system comprised of NT-3 encapsulated in PLGA nanoparticles dispersed in an injectable hydrogel of hyaluronan and methyl cellulose (HAMC). A continuum model was used to fit the *in vitro* release kinetics of an NT-3 analog from a nanoparticle formulation. Interestingly, the model suggested that the linear drug release observed from composite HAMC was due to a diffusion-limiting layer of methyl cellulose on the particle surface. We then studied the effects of processing parameters and excipient selection on NT-3 release, stability, and bioactivity. Trehalose was shown to be the most effective additive for stabilizing NT-3 during sonication and lyophilization and PLGA itself was shown to stabilize NT-3 during these processes. Of four excipients tested, 400 g/mol poly(ethylene glycol) was the most effective during nanoparticle fabrication, with 74% of NT-3 detected by ELISA. Conversely, co-encapsulation of magnesium carbonate with NT-3 was the most effective in maintaining NT-3 bioactivity over 28 days according to a cell-based axonal outgrowth assay. Together, the modeling and optimized processing parameters provide insight critical to designing a controlled bioactive release formulation for ultimate testing *in vivo*.



## 1. Introduction

Spinal cord injury is a devastating condition that affects more than 130,000 people each year worldwide and often results in permanent functional and sensory deficits [1]. Pharmaceutical therapy is promising because many targets for neuroprotection and neuroregeneration have been identified; however, systemic administration is only possible for very few molecules because the blood-spinal cord barrier (BSCB) limits diffusion into the spinal cord. Local delivery is attractive because it bypasses the BSCB, but strategies used clinically are not ideal: external minipumps are prone to infection [2] and bolus injections offer only transient delivery.

A localized drug delivery system comprised of drug-loaded PLGA nanoparticles dispersed within a hydrogel of hyaluronan and methyl cellulose (HAMC) and injected into the intrathecal space that surrounds the spinal cord has been reported [3]. The nanoparticles offer sustained release while the HAMC gel localizes the nanoparticles at the site of injection. The strategy is designed to combine the simplicity and safety of bolus injection with the sustained release offered by pump and catheter systems. Composite HAMC (PLGA nanoparticles embedded in HAMC) is biodegradable/bioresorbable, injectable, and biocompatible in the intrathecal space over 28 days [4]. The HAMC hydrogel itself is also safe, biocompatible, and degraded/eliminated from the intrathecal space [5,6].

The neurotrophins are a family of regenerative proteins that modulate the survival, development, and function of neurons in the central nervous system [7]. A foremost example is neurotrophin-3 (NT-3), which is responsible for the maintenance, proliferation, and differentiation of tyrosine kinase C-positive neurons [8]. NT-3 has been delivered both *in vitro* and *in vivo* using various strategies, including: fibrin scaffolds [9], lipid microtubules embedded in agarose gels [10], transfected olfactory ensheathing cells [11], poly(N-isopropylacrylamide)-co-poly(ethylene glycol) (PNIPAAm-PEG) gels [12], and PLGA microspheres embedded in a PEG gel [13]. NT-3 has been shown to be particularly effective in combination with brain-derived neurotrophic factor (BDNF) [14], cyclic adenosine monophosphate (cAMP) [15], and chondroitinase ABC [10]. Sustained release of NT-3 for 14 days [16] and up to one month [17] has been shown to promote axonal regeneration and functional recovery. The

* Corresponding author at: Donnelly Centre for Cellular and Biomolecular Research, 160 College St., Rm 514 Toronto, ON, Canada M5S 3E1.
*E-mail address:* molly.shoichet@utoronto.ca (M.S. Shoichet).

0168-3659/$ – see front matter © 2012 Elsevier B.V. All rights reserved.
doi:10.1016/j.jconrel.2012.03.024

critical challenge when formulating NT-3 for sustained release from PLGA particles is to retain bioactivity throughout the treatment term.

Proteins in general are susceptible to structural damage when exposed to harsh conditions, including those experienced during encapsulation, release, and storage. For example, during particle synthesis a variety of proteins have been shown to become damaged during sonication [18], lyophilization [19], freeze/thaw cycles [20], and at low pH [21], as summarized in Table 1 (for an extensive review see Ref. [22]). Excipients are often added to drug delivery systems to minimize the damage caused by these processes [19]. For example, lyoprotectants, such as trehalose, are often used to minimize damage during lyophilization [19]; viscosity-controlling agents, such as hyaluronan, have been used to minimize protein denaturation during emulsion processing [23]; and basic additives, such as magnesium carbonate, have been used to neutralize the low pH environment often found inside PLGA particles [24]. These excipients can also unintentionally alter the release profile of proteins from PLGA particles formed by double emulsion, solvent evaporation. Water-soluble additives can act as pore-forming agents and result in faster drug release [25]. Excipients can also modify the solubility of PLGA in the organic phase during processing or alter the osmolarity of the inner aqueous phase, both of which can affect encapsulation efficiency and release kinetics as a result of modified water uptake during nanoparticle solidification [26]. Clearly, it is non-trivial to improve the bioactivity of encapsulated proteins without influencing release kinetics.

Toward the development of a drug delivery system for spinal cord injury, we explore the influence of processing parameters on NT-3 stability, release kinetics, and bioactivity in the context of the proposed PLGA nanoparticle/HAMC hydrogel composite drug delivery system. By fitting experimental data points to a theoretical model of release, we provide insight into the mechanism of NT-3 release from the composite HAMC. NT-3 detection by enzyme-linked immunosorbent assay (ELISA) is used to assess structural damage during processes associated with nanoparticle fabrication, *in vitro* release, and storage. ELISA and a rat dorsal root ganglion bioassay are then used to assess NT-3 release kinetics and bioactivity, respectively, from various PLGA nanoparticle formulations.

## 2. Materials and methods

### 2.1. Materials

Recombinant human NT-3 was purchased from R&D Systems (Minneapolis, USA). Trehalose, $MgCO_3$, lactose, glucose, glycerol, poly-D-lysine, sodium dodecyl sulfate (SDS), bovine serum albumin (BSA), and α-chymotrypsin (type II from bovine pancreas), were purchased from Sigma-Aldrich (Oakville, CA). Poly(DL-lactic-*co*-glycolic acid) 50:50 of inherent viscosity 0.67 dL/g (Mn = 30,000, Mw = 45,000) was purchased from Durect (Cupertino, USA). Poly(vinyl alcohol), 6000 g/mol was purchased from Polysciences Inc. (Warrington, USA). Sodium hyaluronate, 2600 kg/mol was purchased from Lifecore (Chaska, USA). Methyl cellulose, 300 kg/mol, was purchased from Shin-Etsu (Tokyo, Japan). Sodium hydroxide was purchased from EMD Chemicals (Gibbstown, USA). Pluronic F-127 was purchased from BASF (Mississauga, CA). Fetal bovine serum (FBS), B-27 serum-free supplement, penicillin–streptomycin, and laminin were purchased from Invitrogen (Burlington, CA).

Artificial cerebrospinal fluid (aCSF) at a pH of 7.4 was prepared as described by Jimenez Hamann et al., and was composed of 148 mM NaCl, 3 mM KCl, 0.8 mM $MgCl_2$, 1.4 mM $CaCl_2$, 1.5 mM $Na_2HPO_4$, and 0.2 m M $NaH_2PO_4$ [27]. High performance liquid chromatography (HPLC) grade dichloromethane (DCM), dimethyl sulfoxide (DMSO), tetrahydrofuran (THF), and hydrochloric acid (HCl) were purchased from Caledon Labs (Georgetown, CA). Dulbecco's phosphate buffered saline (pH 7.4, 9.55 g/L) was purchased from Wisent Inc. (St-Bruno, CA). All buffers were prepared using water distilled and deionized using a Millipore Milli-RO 10 Plus and Milli-Q UF Plus at 18 MΩ resistance (Millipore, Bedford, USA). Neural basal media and glutamine 200 mM were purchased from Gibco (Burlington, CA).

### 2.2. Nanoparticle processing and hydrogel preparation

NT-3 loaded nanoparticles were prepared using a water/oil/water (w/o/w) double emulsion solvent evaporation technique, as described previously [3]. Briefly, an inner aqueous phase of 100 μL aCSF containing 5 μg NT-3 and 12 mg BSA was mixed with an organic phase of 0.9 mL DCM, 120 mg PLGA and 0.45 mg Pluronic F-127. This mixture was sonicated using a Vibra-Cell (Sonics, Newtown, USA) on ice for 10 min at 26 W and 20 kHz to create the primary emulsion, which was subsequently mixed with the outer aqueous phase of 5.5 mL of 25 mg/mL poly(vinyl alcohol) (PVA). The secondary emulsion was formed through sonication on ice for an additional 10 min at 39 W and 20 kHz. This double emulsion was then added to 34.5 mL of 25 mg/mL PVA and stirred gently for 20 h at room temperature. PLGA nanoparticles were then isolated and washed 4 times by ultracentrifugation (Beckman, Mississauga, CA), lyophilized in a Freezone 6 with a vacuum collector operating at 10 Pa and −52 °C (Labconco, Kansas City, USA), and stored at −20 °C. Various excipients were also incorporated in modified formulations: (a) 14 mg trehalose and 1.3 mg hyaluronan were dissolved in the inner aqueous phase; (b) 5 μL of PEG 400 was added to the inner aqueous phase; (c) 12 mg of α-chymotrypsin was used in place of NT-3 and BSA in the inner aqueous phase; (d) 4 mg $MgCO_3$ was added to the organic phase.

HAMC hydrogels were prepared through the physical blending of hyaluronan and methyl cellulose in aCSF for a final composition of 1 wt.% 2600 kg/mol hyaluronan and 3 wt.% 300 kg/mol methyl cellulose. Methyl cellulose and hyaluronan were sequentially dispersed in aCSF using a dual asymmetric centrifugal mixer (Flacktek Inc., Landrum, USA) and left to dissolve overnight at 4 °C.

### 2.3. Nanoparticle characterization

Particle size was measured using dynamic light scattering (Zetasizer Nano ZS, Malvern Instruments, Malvern, UK). Particle yield was defined as the total mass of particles produced divided by the initial mass of PLGA used, adjusted for protein content and assuming negligible PVA content. Drug loading is the mass fraction of NT-3 (or α-chymotrypsin) in the particles, while encapsulation efficiency is the measured drug loading of the particles divided by the theoretical maximum drug loading. To determine the total protein encapsulation efficiency, 1 mg of nanoparticles was dissolved in 5 mL DMSO and added to 5 mL of 0.05 M NaOH containing 0.05 wt.% SDS and analyzed using the total protein bicinchoninic acid (BCA) assay according to the manufacturer's instructions (Thermo Scientific, Nepean, CA). To determine NT-3 encapsulation efficiency, 1 mg of particles was dissolved in 1 mL DCM for 1 h, conditions that were not found to affect the detected concentration of control NT-3 by ELISA. The protein was then extracted into a liquid phase of 10.5 mL 0.1% BSA in PBS and analyzed using an NT-3 ELISA (R&D Systems, Minneapolis, USA) according to the

**Table 1**
A summary of several causes of protein destabilization during *in vitro* processing, drug release, and storage.

| | Processing | Drug release | Storage |
|---|---|---|---|
| Potential causes of protein instability | Lyophilization | Aggregation | Incubation |
| | Sonication<br>Organic solvents | Adsorption<br>Denaturation<br>Degradation | Freeze/thaw cycles |

manufacturer's protocol. In both instances the drug payload was calculated using the equation:

$$\frac{M_d^{protein}}{M_s^{particle}} \quad (1)$$

In Eq. (1), $M_d^{protein}$ is the mass of protein detected (by ELISA or BCA) and $M_s^{particle}$ is the mass of particles used in the assay (1 mg). Encapsulation efficiency, EE, was calculated using the equation:

$$EE = \left[ \frac{\frac{M_d^{protein}}{M_s^{particle}}}{\frac{M_t^{protein}}{M_t^{particle}}} \right] \times 100\% \quad (2)$$

Eq. (2) is actual drug payload (Eq. (1)) divided by theoretical maximum drug payload, expressed as a percent. $M_t^{protein}$ is the total mass of protein used in the particle synthesis and $M_t^{particle}$ is the theoretical maximum particle yield.

### 2.4. NT-3 release study

Release profiles of α-chymotrypsin or NT-3 from each particle batch were obtained by dispersing 10 mg of particles in 0.1 mL of HAMC in a 2 mL microcentrifuge tube (Axygen, Union City, USA) using a dual asymmetric centrifugal mixer at 3300 rpm for 4 min to produce a final composition of 8 wt.% particles, 1 wt.% hyaluronan, and 3 wt.% methyl cellulose. The composite was then warmed to 37 °C and 0.9 mL prewarmed aCSF was added to the sample tubes. The supernatant was removed and replaced completely at the following time points: 3, 6 h, 1, 3, 7, 14, 21, and 28 d. The protein content of the supernatant was determined by ELISA (NT-3) or BCA (α-chymotrypsin). After 28 d, the NT-3 remaining inside the particles was quantified by dissolving the particles in 0.1 mL DCM and extracting the remaining protein into 1 mL reagent diluent for protein quantification by ELISA.

### 2.5. Mathematical model

A mathematical model, constructed in Matlab (MathWorks, Natick, USA), was used to quantitatively describe the effect of various processing parameters on the release kinetics of α-chymotrypsin, an analog for NT-3. Applying the models developed by Faisant et al. [28] and Raman et al. [29], with minor modifications (Supplemental information), release from composite HAMC was simulated in two parts: release from PLGA particles was simulated using a one-dimensional Fickian diffusion model in spherical coordinates and release from the HAMC hydrogel was simulated using a one-dimensional Fickian diffusion model in Cartesian coordinates. In the published model a diffusivity term describes the dependence of protein diffusion through the PLGA matrix during the degradation controlled portion of the release profile. Our modification was to apply a fit parameter to this diffusivity term which accounted for the presence of an adsorbed methyl cellulose layer on the surface of the PLGA particle. The fit parameter functions to de-emphasize the contribution of PLGA degradation to protein release. We previously reported the interaction of methyl cellulose with the surface of dispersed nanoparticles resulted in unusual, near zeroth order release kinetics, but until now had not modeled the system [30]. We suggest that adding the fit parameter is more appropriate than simplifying the model because although PLGA matrix degradation does not control protein release in the HAMC system, the polymer degrades as predicted (Fig. 2).

### 2.6. PLGA degradation

To determine whether dispersion in HAMC altered the rate of PLGA degradation relative to dispersion in aCSF, 10 mg of PLGA particles (without encapsulated protein) was dispersed in 0.1 mL concentrated HAMC or aCSF in 2 mL microcentrifuge tubes. In both cases, 0.9 mL aCSF was added to all tubes and incubated at 37 °C on a rotary shaker at 2 Hz. Samples were washed 6 times with ice-cold distilled water, isolated by ultracentrifugation, and lyophilized at the following time points: 0, 2, 4, 8, 21, and 30 d. The molecular weight of the PLGA samples was determined by gel permeation chromatography in THF relative to polystyrene standards on a system comprised of two-column sets, GMHHR-M and GMHHR-H (Viscotek, Worcestershire, UK), and a triple detector array (TDA302) at room temperature with an eluent flow rate of 0.6 mL/min.

To determine fractional mass loss of PLGA, each sample was weighed before and after incubation and processing. Mass loss values were corrected by the amount of mass loss at day 0 to account for losses resulting from the isolation process.

### 2.7. Detection of NT-3

The capture antibody used in the NT-3 ELISA kit binds an epitope of folded recombinant human NT-3. Concentrations measured by ELISA were therefore interpreted as a measure of the tertiary structure of NT-3.

#### 2.7.1. The effect of nanoparticle fabrication, sonication, and lyophilization on NT-3

To determine the effect of double emulsion processing on NT-3 detection, nanoparticle formulations were dissolved and analyzed by NT-3 ELISA and BCA. The fraction of NT-3 which retained its native conformation was taken as the ratio of the encapsulation efficiency in PLGA of NT-3 (ELISA) to that of BSA + NT-3 (BCA) under the assumption that total NT-3 and BSA encapsulation efficiencies were similar.

To study the effect of sonication on NT-3 detection, samples of 1 mL of 1 ng/mL NT-3 in aCSF were sonicated for 5 min, 10 min, or 10 min with 400 mM trehalose at 26 W and 20 kHz to simulate the conditions used to create the primary emulsion. The concentration of NT-3 was then measured by ELISA.

To assess the effect of lyophilization on NT-3, 0.9 mL of 1 ng/mL NT-3 was combined with different potential lyoprotectants at 400 mM in 0.5 mL aCSF in 2 mL microcentrifuge tubes, lyophilized for 3 d, reconstituted in reagent diluent and assayed by ELISA. The following agents were studied: trehalose, lactose, cyclodextrin, galactose, glucose, and glycerol.

#### 2.7.2. Effect of pH on NT-3 bioactivity

Samples of 1 ng/mL NT-3 were incubated for 24 h at 37 °C in aCSF with a pH of: 7.4, 6.0, 4.0, 3.0, or 2.0. The concentration of NT-3 in the samples was then determined by ELISA and the results normalized to the sample at pH 7.4.

#### 2.7.3. Effect of storage conditions on NT-3 bioactivity

The effect of different storage conditions on NT-3 bioactivity was examined by storing 1 mL of 667 pg/mL NT-3 in aCSF at 4 °C or at −80 °C, with and without the addition of 1 wt.% BSA for 7 days. An incubation study at 37 °C of 1 ng/mL NT-3 in aCSF was carried out for a total of 30 d with samples collected after: 1, 2, 4, 7, 14, 23, and 30 d.

### 2.8. NT-3 bioactivity by dorsal root ganglia (DRG) bioassay

The bioactivity of NT-3 released over 28 d was determined using a DRG bioassay performed as described by Hurtado et al. [31] and Blits et al. [32], with modifications described below. All animal procedures were performed in accordance with the Guide to the Care and Use of Experimental Animals (Canadian Council on Animal Care) and protocols were approved by the Animal Care Committee of the Research Institute of the University Health Network. Rat embryo DRG (E17 female Sprague–Dawley rats) were removed and pooled in differentiation media comprised of neural basal media with 1 vol.% fetal bovine serum, 2 vol.% B-27 serum-free supplement, 1 vol.% penicillin–streptomycin,

1 vol.% L-glutamine. The DRG were then placed on 12 mm diameter glass cover slips coated with poly-D-lysine (50 μg/mL in sterile water) and laminin (5 μg/mL in PBS) in a 24-well plate. All wells were treated with 0.5 mL of differentiation media and 0.5 mL of the NT-3 release study supernatant, which was collected at 3, 6 h, 1, 3, 7, 14, 21, and 28 d. For the controls, 0.5 mL differential media and 0.5 mL of aCSF with appropriate concentrations of NT-3 were added to the wells. The DRG were grown for 48 h at 37 °C and 5% $CO_2$, and imaged using a CoolSnap HQ camera (Photometrics, Tucson, USA) mounted on an Axiovert S100 microscope (Zeiss, Toronto, CA). Neurites greater than 50 μm were counted for 10 DRG per group. Treatment groups were compared to NT-3 controls to assess bioactivity as previously reported [31–33].

### 2.9. Statistical analysis

All data are presented as mean ± standard deviation. For pair-wise comparison of these averages, t-tests were carried out. For comparison of multiple groups, ANOVA comparisons were conducted and when differences were found between groups, Bonferroni *post-hoc* analysis was performed. Studies reported in Figs. 1–6 are $n = 3$ and the DRG assay reported in Fig. 7 was $n = 10$. Significance was assigned at $p < 0.05$ unless otherwise specified.

## 3. Results

### 3.1. Effect of embedding PLGA nanoparticles in HAMC

The release of α-chymotrypsin, a model protein for NT-3, from the composite hydrogel was compared to each of PLGA alone and HAMC alone (Fig. 1). Release from HAMC alone was fastest and near completion within 1 d, demonstrating a diffusion-controlled mechanism. Release from PLGA nanoparticles showed the typical burst release within the first 2–3 d, followed by a plateau. Unexpectedly, release from the composite hydrogel deviated significantly from the controls, having a significantly reduced burst release followed by a linear release profile, suggesting an interaction between PLGA and HAMC. We hypothesized that one of two mechanisms was causing this behavior: (a) embedding the PLGA in HAMC reduced the degradation rate of the particles, resulting in an altered release profile; or (b) the MC in HAMC adsorbed to the surface of the PLGA particles, thereby resulting in reduced diffusion across the PLGA–hydrogel boundary and an altered release profile.

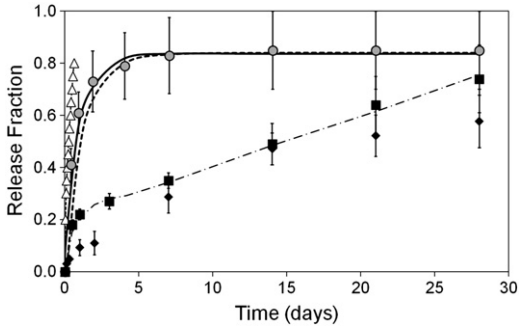


**Fig. 1.** Embedding PLGA nanoparticles in HAMC reduces the burst release and supports sustained delivery of α-chymotrypsin, an analog for NT-3. Release of α-chymotrypsin from (■) PLGA nanoparticles embedded in HAMC had a lower burst release and more sustained delivery than from ● PLGA nanoparticles alone. These two data sets were previously published by Baumann et al. [3]. α-Chymotrypsin release from (Δ) HAMC alone occurs over the span of hours. A continuum model based on Fickian diffusion was able to predict release from ( ) PLGA nanoparticles in aCSF and from ... HAMC; however, a similar model that incorporated diffusion through the HAMC gel was not able to predict release from (–) nanoparticle embedded in HAMC. Only when model variables associated with the particles themselves were augmented was an accurate fit obtained — ·. Release of α-chymotrypsin and its model fit was in close agreement with a similar formulation with encapsulated (♦) NT-3 in PLGA nanoparticles, embedded in HAMC.

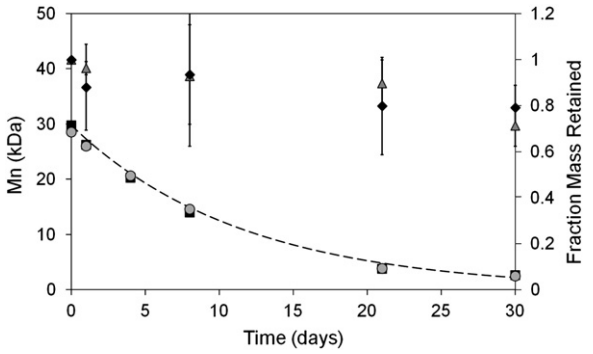


**Fig. 2.** Attenuation of the burst release from composite HAMC is not the result of altered PLGA nanoparticle degradation. PLGA degradation was monitored over 30 d by organic GPC for ● PLGA nanoparticles in aCSF and (■) PLGA nanoparticles embedded in HAMC. Both traces were similar to each other and to a (–) first order degradation model using $k_{deg} = 0.086\ days^{-1}$. Mass loss for ▲ PLGA nanoparticles in aCSF and (♦) PLGA nanoparticles embedded in HAMC were indistinguishable.

To better understand how embedding the particles in HAMC reduced drug release, the release data was simulated in Matlab. Release of α-chymotrypsin from a 3 mm slab of HAMC alone was described with a one-dimensional Fickian diffusion model in Cartesian coordinates with a good fit ($R^2 = 0.99$) and molecular diffusivity of $8.6 \times 10^{-7}\ cm^2/s$ (Fig. 1). Similarly, release from PLGA nanoparticles in aCSF was fit using a modified one-dimensional Fickian diffusion model in spherical coordinates ($R^2 = 0.96$) by the following model parameters: a burst fraction ($F_{burst}$) of 0.85, an initial diffusivity ($D_o$) of $8.9 \times 10^{-18}\ cm^2/s$, and a fit parameter (k) of 1. When these two models were combined to simulate release from PLGA nanoparticles embedded in HAMC, the resulting fit was poor ($R^2 = -1.05$) and resembled a slightly delayed release from PLGA nanoparticles. Only when the model parameters of the nanoparticles were adjusted to $F_{burst} = 0.3$, $D_o = 8.9 \times 10^{-17}\ cm^2/s$, and $k = 1.9 \times 10^{15}$ were the experimental data well described ($R^2 = 0.99$). While acknowledging that diffusivity can be affected by multiples parameters, we note that the diffusivity values obtained using the model are in good agreement with the previously published drug diffusivity value of $3 \times 10^{-17}\ cm^2/s$ for chondroitinase ABC from PLGA nanospheres [34]. The release kinetics of α-chymotrypsin and the fit produced by the mathematical model were similar to release kinetics of NT-3 under identical formulation and release conditions (Fig. 1). The similarity in release profile for the model protein α-chymotrypsin and NT-3 was expected because α-chymotrypsin and NT-3 have similar molecular weights (25 kDa and 29 kDa) and isoelectric points (8.8 and 9.4).

To elucidate the impact of the HAMC on the degradation rate of PLGA, the changes in molar mass (by GPC) and mass were followed over 30 d for PLGA in HAMC *vs.* PLGA in aCSF buffer. As shown in Fig. 2, the change in molar mass for PLGA was unaffected by the presence of HAMC and both degradation profiles are well described by a first-order degradation model using a degradation rate constant ($k_{deg}$) of $0.086\ d^{-1}$, in close agreement with published values of PLGA degradation between $0.075\ d^{-1}$ and $0.093\ d^{-1}$ [35]. Similarly, mass loss of PLGA particles in aCSF was indistinguishable from PLGA particles dispersed in HAMC over 30 d.

### 3.2. NT-3 stability improvement

Beyond sustained release, NT-3 stability was investigated because damage to tertiary protein structure is a common concern in polymeric sustained release devices. Excipients are often added to PLGA particles to stabilize encapsulated proteins against the conditions encountered in particle synthesis [22]. To maximize the fraction of NT-3 with native tertiary structure upon release from PLGA nanoparticles, we conducted a life-cycle analysis and isolated the fabrication steps expected to affect NT-3 structure.

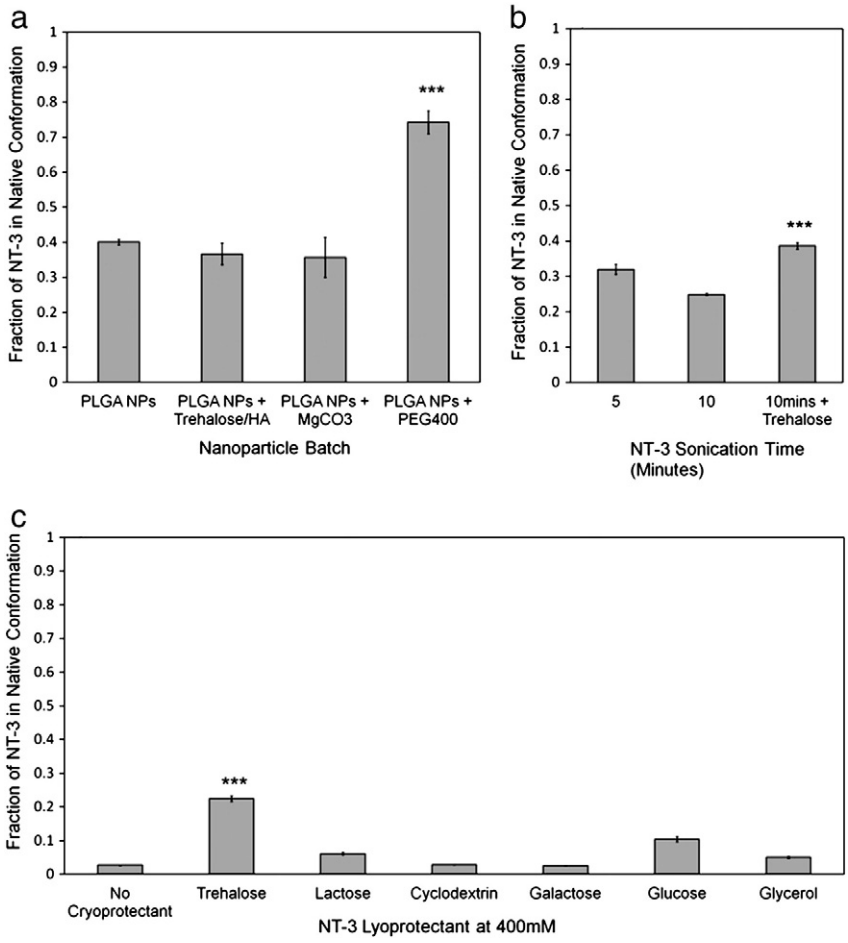


**Fig. 3.** The effects of three processing steps on the stability of NT-3 were investigated by ELISA. (a) Encapsulation of NT-3 within PLGA nanoparticles stabilized the protein during the double emulsion synthesis, retaining approximately 40% of detectable NT-3 using the following co-encapsulants: trehalose + hyaluronan, $MgCO_3$, or no additives. Co-encapsulated PEG 400 significantly improved NT-3 stability ($p<0.001$, $n=3$), resulting in 74% detection after processing. (b) After sonication 400 mM trehalose significantly improved NT-3 detection from 25% to 39% ($p<0.001$, $n=3$). (c) The addition of 400 mM trehalose prior to lyophilization improved NT-3 detection significantly compared to all other additives. *** = $p<0.001$ ($n=3$).

*3.2.1. Structural damage during nanoparticle fabrication*

We first examined the effect of excipients on NT-3 detection by ELISA after nanoparticle fabrication. After double emulsion synthesis, 40% of the NT-3 encapsulated in PLGA nanoparticles was detected (Fig. 3a). Trehalose and hyaluronan were co-encapsulated within PLGA nanoparticles because trehalose is a known lyoprotectant and hyaluronan is known to improve encapsulated protein stability by increasing the viscosity of the inner aqueous phase of the emulsion, reducing contact between the protein and the organic solvent during processing [23]. Surprisingly, there was no improvement in NT-3 detection after co-encapsulation, likely because PLGA masks any improvement by acting through the same stabilization mechanisms as trehalose and hyaluronan. Magnesium carbonate was also screened as a co-encapsulant to improve the long-term stability of NT-3, where the

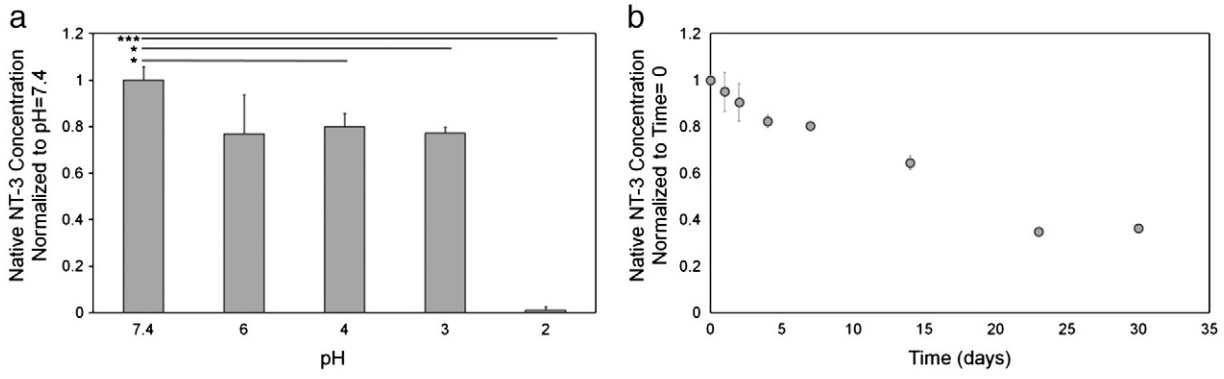


**Fig. 4.** NT-3 was not detected by ELISA after exposure to low pH and its detection reduced over time after incubation at 37 °C. (a) NT-3 detection by ELISA was fairly stable between pH 7.4 and pH 3 when incubated for 24 h; however, below pH 3 NT-3 was not detected. (b) The ELISA detection of NT-3 steadily reduced at approximately 2.5% per day over the first 23 d of incubation at 37 °C in aCSF. * = $p<0.05$, ** = $p<0.01$, *** = $p<0.001$.

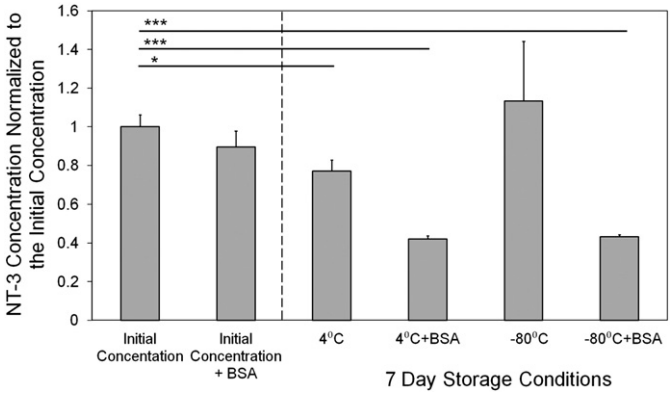


**Fig. 5.** NT-3 stored at 4 °C or −80 °C remained stable for 7 d, but not when stored at 4 °C with 1 wt.% BSA. When NT-3 was stored in aCSF for 7 d at −80 °C, the NT-3 concentration measured by ELISA was similar to the initial concentration. Similarly storage at 4 °C only resulted in a modest 19% loss in detection compared to the initial concentration ($p<0.05$, $n=3$, mean ± standard deviation). However, when stored at these temperatures in the presence of 1 wt.% BSA, more than half of the initial NT-3 detected was lost ($p<0.001$, $n=3$, mean ± standard deviation). A fresh sample in 1 wt.% BSA (initial concentration + BSA) did not exhibit this same loss in detection, which indicates that this phenomenon is not simply due to the BSA blocking the ELISA plate. * = $p<0.05$, ** = $p<0.01$, *** = $p<0.001$.

carbonate ion is known to buffer the acidic degradation products of PLGA [36]. Magnesium carbonate did not affect initial NT-3 stability, as expected, because the acidic microenvironment within PLGA takes time to develop. Neither trehalose + hyaluronan nor magnesium carbonate impacted the amount of NT-3 detected; however, addition of PEG 400 had a profound impact, with 74% of NT-3 detected, likely because PEG 400 is a surfactant that minimizes contact between NT-3 in the inner aqueous phase and the organic phase during the high energy sonication required for particle formation [37].

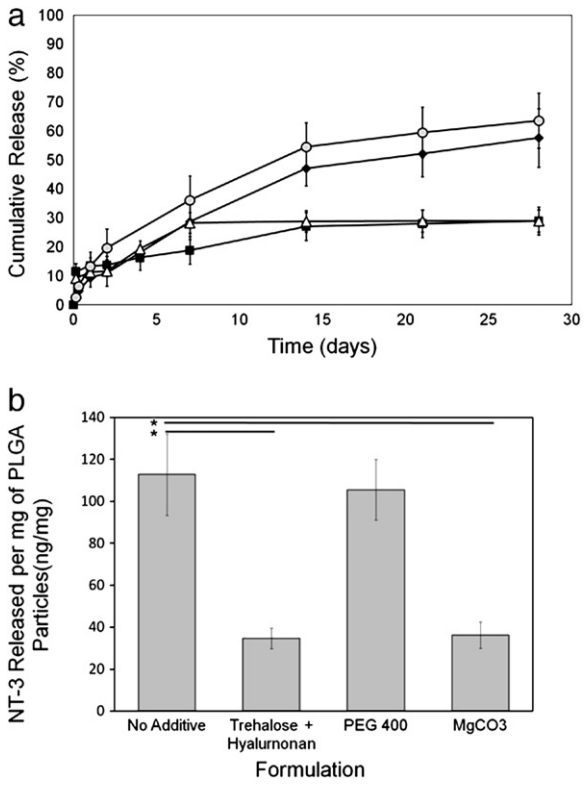


**Fig. 6.** NT-3 *in vitro* release from PLGA nanoparticles was fine-tuned by incorporating excipients and adjusting polymer properties. (a) NT-3 release from PLGA nanoparticles embedded in (♦) HAMC was not considerably changed by co-encapsulation with trehalose and hyaluronan. Co-encapsulation with (■) $MgCO_3$ resulted in a reduced burst and reduced cumulative release of NT-3. Co-encapsulation with (Δ) PEG 400 led to a 7 d release profile, with only 1% released thereafter. (b) Cumulative 28 d released amounts of NT-3 per mg of PLGA nanoparticle for all four formulations, was largest from PLGA alone and PLGA with PEG 400. This demonstrates that approximately 100 ng of NT-3 can be delivered over 7 d from the formulation with PEG 400, while 110 ng of NT-3 can be delivered over 28 d from the formulation without additives. All NT-3 concentrations were determined by ELISA. * = $p<0.05$.

The effects of sonication and lyophilization on NT-3, two key operations used to create nanoparticles in the double emulsion procedure, were then investigated. NT-3 was particularly sensitive to sonication, as only 32% and 25% of NT-3 were detected after sonicating for 5 and 10 min, respectively (Fig. 3b). Sonication of an NT-3 solution containing 400 mM trehalose for 10 min yielded 39% detection (compared to 25% without trehalose), an effect which is likely caused by the reduction in cavitation associated with the increased viscosity afforded by trehalose [38]. NT-3 was also highly susceptible to lyophilization. In aCSF, only 3% of the lyophilized NT-3 was measured by ELISA. Of the several lyoprotectants investigated (Fig. 3c), only 400 mM trehalose was able to improve NT-3 detection from 3% to 22%, whereas all other agents yielded detection below 10% (Fig. 3c). The most likely mechanism for this protective effect is that trehalose is able to satisfy the hydrogen bonding requirements of polar groups on the exposed surface of NT-3 after the sublimation of water [39].

### 3.2.2. Structural damage during drug release

The effects of pH and long-term incubation on NT-3 were studied to determine whether the tertiary structure was sensitive to environments encountered during *in vitro* release studies. NT-3 dissolved in aCSF and incubated at 37 °C was stable for 24 h at pH 7.4. Moreover, 80% of NT-3 was detected between pH 3 and pH 6 for 24 h; however, at pH 2, effectively all NT-3 was denatured, as only 1% of the initial concentration was detected by ELISA (Fig. 4a). This dramatic loss of NT-3 may be due to charge induced destabilization of the homodimer or cleavage of the protein itself; however, the exact mechanism was not investigated.

During release studies, NT-3 diffused from composite HAMC into the supernatant where it remained at pH 7.4 and 37 °C for up to 7 d, which was the maximum interval between sampling. Under these conditions, 80% of NT-3 was detected after 7 d. This value decreased to 35% after 23 d (Fig. 4b). Reflecting the complexity of the experimental system, the data reported in Fig. 6 has not been normalized to account for this 20% loss of NT-3 (over 7 days) because it was not known if freshly prepared NT-3 solution and released NT-3 would respond identically to incubation. We instead interpret the stability data in Fig. 4b to show that the data in Fig. 6 is an underestimate of the actual percent of NT-3 released.

### 3.2.3. Structural damage during storage

Samples of NT-3 containing 0.1 wt.% BSA in solution were stored for 7 d at 4 °C and at −80 °C with and without the addition of additional 1 wt.% BSA. Storage at both temperatures largely maintained NT-3 conformation over this time period, but the addition of 1 wt.% BSA significantly reduced the detection of the NT-3 (Fig. 5). BSA, a larger and more flexible protein than NT-3, was added to NT-3 to improve its stability based on the assumption that BSA would preferentially adsorb onto the surface of the storage vessel, thereby limiting NT-3 loss due to adsorption and denaturation [40]; however, surprisingly, approximately half of the NT-3 originally detected was lost. This was true at both 4 and −80 °C. Importantly, we know that the additional BSA did not block the ELISA capture antibody because when 1 wt.% BSA was added to a fresh sample of NT-3, all of the original NT-3 was detected. The 4 and −80 °C result is counterintuitive because protein stability often increases with concentration, but there is evidence in the literature for thermal cycling induced aggregation of BSA, and that this effect is more significant at higher protein concentration [41]. Within this environment thiol-disulfide interchange may account for the co-aggregation of NT-3 [42]. This hypothesis can be tested by including the disulfide bond reducing reagent dithiothreitol,

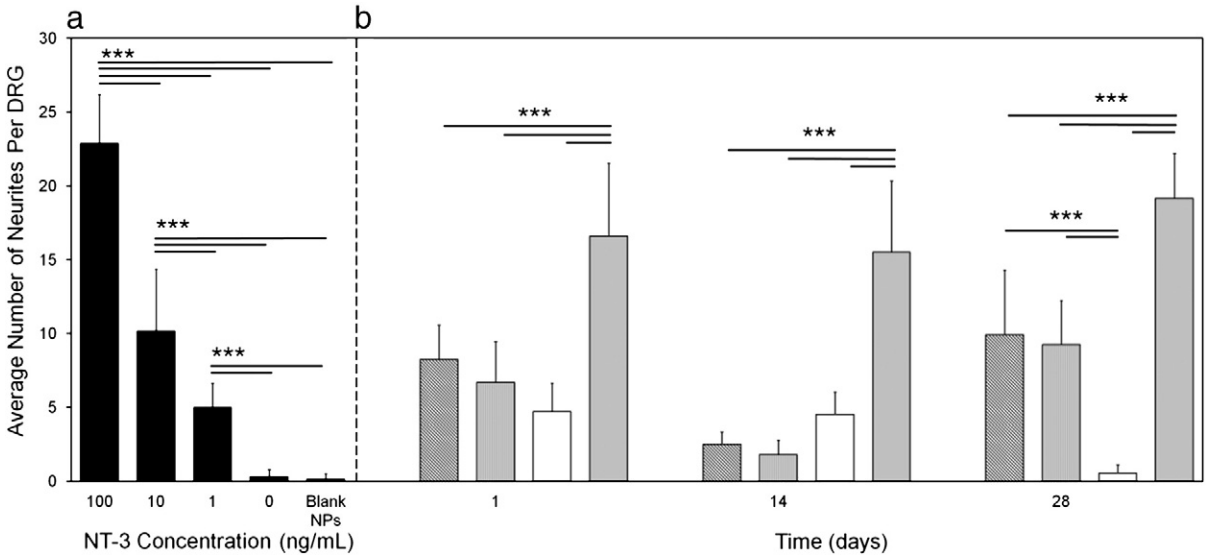


**Fig. 7.** Released NT-3 is bioactive in a rat dorsal root ganglia neurite outgrowth assay. (a) NT-3 standards in 0.5 mL aCSF and 0.5 mL differentiation media. The increase in average number of neurites/DRG with increased NT-3 suggests a correlation in amount of NT-3 present and number of neurites. (b) The NT-3 released from PLGA nanoparticles was followed in terms of the following co-encapsulants: ▨no additives, trehalose ▥ and hyaluronan, (□) PEG 400, and ▩ $MgCO_3$. All samples up to 28 days stimulated neurite outgrowth from rat dorsal root ganglia, with the exception of the PEG 400 batch at day 28. Batches with co-encapsulated $MgCO_3$ exhibited more robust neurite outgrowth with significant differences relative to all other variables at 1 d, 14 d, and 28 d. * = $p<0.05$, ** = $p<0.01$, *** = $p<0.001$ ($n=10$, mean ± standard deviation).

which prevents intermolecular disulfide bond formation, in future stability studies.

### 3.3. Effect of processing parameters on NT-3 release kinetics

Excipients can alter release kinetics by acting as pore-forming agents or by changing the particle formation process [43]. Consequently, the effects of additives on NT-3 release kinetics from PLGA nanoparticles embedded in HAMC were investigated and are reported in Fig. 6. The release curves in Fig. 6 are total release as detected by ELISA, that is, all NT-3 with an intact ELISA binding epitope, which includes both bioactive NT-3 and partially denatured protein. ELISA was selected because it is quantitative, while the cell assay described in the following section is semi-quantitative. NT-3 was separately co-encapsulated with one of: trehalose and hyaluronan, $MgCO_3$, or PEG 400. In each synthesis, particle yield was between 67% and 85%, nanoparticles were 200–300 nm in diameter and PDI (polydispersity index) was between 0.08 and 0.15. None of the excipients tested was found to affect nanoparticle yield or diameter; however, the encapsulation efficiency was affected. Total protein encapsulation was: 97% without an excipient, 98% when co-encapsulated with PEG 400, 70% with $MgCO_3$, and 30% with trehalose and hyaluronan. These encapsulation efficiencies correspond to total protein loadings of: 8.8 wt.%, 8.9 wt.%, 6.4 wt.%, and 2.7 wt.%, respectively.

Notwithstanding significant differences in encapsulation efficiency, the release profile of NT-3 from PLGA nanospheres dispersed in HAMC when co-encapsulated with trehalose + hyaluronan *vs.* excipient-free control nanoparticles was similar, with 63% ± 9% and 57% ± 10% cumulative release after 28 d, respectively (Fig. 6a). Interestingly, NT-3 co-encapsulated with either $MgCO_3$ or PEG 400 resulted in a lower cumulative release of only 28% ± 10% over 28 d, with very little additional NT-3 released from co-encapsulated PEG 400 after 7 d. The total mass of NT-3 released was 113 ± 19 ng NT-3/mg particle for the formulation with no additives, 34 ± 5 ng NT-3/mg particle for the trehalose + hyaluronan formulation, 105 ± 15 ng NT-3/mg particle for the PEG 400 formulation, and 36 ± 6 ng NT-3/mg particle for the $MgCO_3$ batch (Fig. 6b). Note that in no formulation did the PLGA particles enter the third phase of release, matrix collapse, in agreement with the relatively minor reduction in molecular weight over time found by GPC (Fig. 2). These data suggest that the most NT-3 released over a 28 d period is achieved from both PLGA nanoparticles encapsulated with no additives and those with PEG 400. For the no additive formulation, the large payload results from the efficient release of encapsulated NT-3, with reference to the total encapsulation efficiency and intact NT-3 detected by ELISA (Fig. 3a). For the PEG containing formulation, a similar NT-3 payload was achieved despite less efficient delivery, ~30% of total *vs.* ~60% of total for the no excipient formulation after 28 days. The similar NT-3 payload of ~110 ng/mg is derived from an increased proportion of intact NT-3 (Fig. 3a).

### 3.4. In vitro bioactivity

The bioactivity of NT-3 released from composite HAMC was measured by a semi-quantitative neurite outgrowth assay using embryonic rat DRGs. Unlike the NT-3 ELISA, the DRG detect only native growth factor. These DRG demonstrated a dose response to NT-3 between 1 and 100 ng/mL where the number of neurites increased with increasing NT-3 concentration, which is consistent with previous reports [44]. At days 1, 14, and 28, all nanoparticle formulations promoted neurite outgrowth except for the formulation that co-encapsulated PEG 400 (Fig. 7). In this case, no neurite outgrowth was observed at 28 d because there was no NT-3 released between 14 and 28 d for this formulation, which is substantiated by the ELISA data.

The control nanoparticle formulation and the batch that had trehalose and hyaluronan co-encapsulated were statistically indistinguishable at all time points, which suggests that any bioactivity improvement caused by these additives was marginal and undetectable by the DRG bioassay. The batch containing PEG 400 also elicited similar DRG neurite outgrowth up to 14 d compared to the aforementioned samples, but at 28 d the bioactivity of the NT-3 in the supernatant was identical to the control. The nanoparticle batch containing co-encapsulated $MgCO_3$ exhibited significantly more robust neurite outgrowth than all other nanoparticle batches at all time points, which demonstrates that even with the reduced amount of NT-3 released, more of it was bioactive. This effect is most evident at 28 d, when the amount of NT-3 detected by ELISA was very small, yet exerted a potent effect on the DRG. This result underscores the importance of determining the bioactivity of released proteins as a complement to ELISA, which detected NT-3 with an intact

ELISA binding epitope. It is clear from the divergent ELISA and DRG data that the ELISA binding epitope and ligand binding site are distinct, and that NT-3 detected by ELISA is not necessarily biologically active. Representative pictures of the DRG for each formulation are shown in Fig. 8.

## 4. Discussion

NT-3 is a neuroregenerative protein that modulates the maintenance, proliferation, and differentiation of neurons that express TrkC receptors [8] and has been investigated pre-clinically as a treatment for spinal cord injury and stroke. Sustained release of NT-3 has resulted in improved tissue and functional benefit relative to instantaneous release in the treatment of spinal cord injury, where NT-3 was released for 14 d [16] and 28 d [17]. Given the lack of FDA-approved methods for localized and sustained release for treatment of acute SCI, we sought to formulate our experimental drug delivery system [3] for release of NT-3.

A principal challenge of formulating proteins for sustained release is maintaining bioactivity over the desired treatment term. There is substantial literature on sustained release from PLGA particles [45], and while sustained NT-3 release from PLGA microparticles embedded in a PEG gel has been published, bioactivity was not measured [13]. One property of PLGA particles that is well described is the formation of an acidic microenvironment within the particle during hydrolytic degradation [36]. We were concerned that embedding PLGA particles in HAMC may increase the acidity of the PLGA environment by impeding the diffusive release of acidic oligomers. To better understand the interaction between PLGA particles and HAMC, we fitted experimental release data using a mathematical model and monitored the degradation kinetics and mass loss of PLGA.

The release of dissolved α-chymotrypsin from HAMC alone was well described by Fickian diffusion in Fig. 1 and release from PLGA particles was likewise well described by a one-dimensional Fickian diffusion model in spherical coordinates with a time-dependent diffusivity term. However, the release of encapsulated α-chymotrypsin from composite HAMC could not be described using a model incorporating the best fit parameters from the freely-suspended particles and Fickian diffusion in HAMC, suggesting that diffusion through the PLGA nanoparticles and HAMC are not distinct processes. This model only accurately described the composite HAMC release profile of α-chymotrypsin and NT-3 after the particle model parameters were adjusted dramatically. The revised model parameters suggest that because such a large empirical fit parameter is required to describe release from the system, there is another physical mechanism controlling release besides the diffusion and particle degradation considered by the model. Together with the observation in Fig. 2 that the molecular weight and mass loss of PLGA are not influenced by the presence of HAMC, and that the mathematical models demonstrate that diffusion through HAMC is not the source of delayed release, we suggest that an interaction between HAMC and PLGA nanoparticles is creating a diffusive barrier at the particle–hydrogel interface. Since methyl cellulose gels through hydrophobic junctions [46] and methyl cellulose and PLGA particles associate

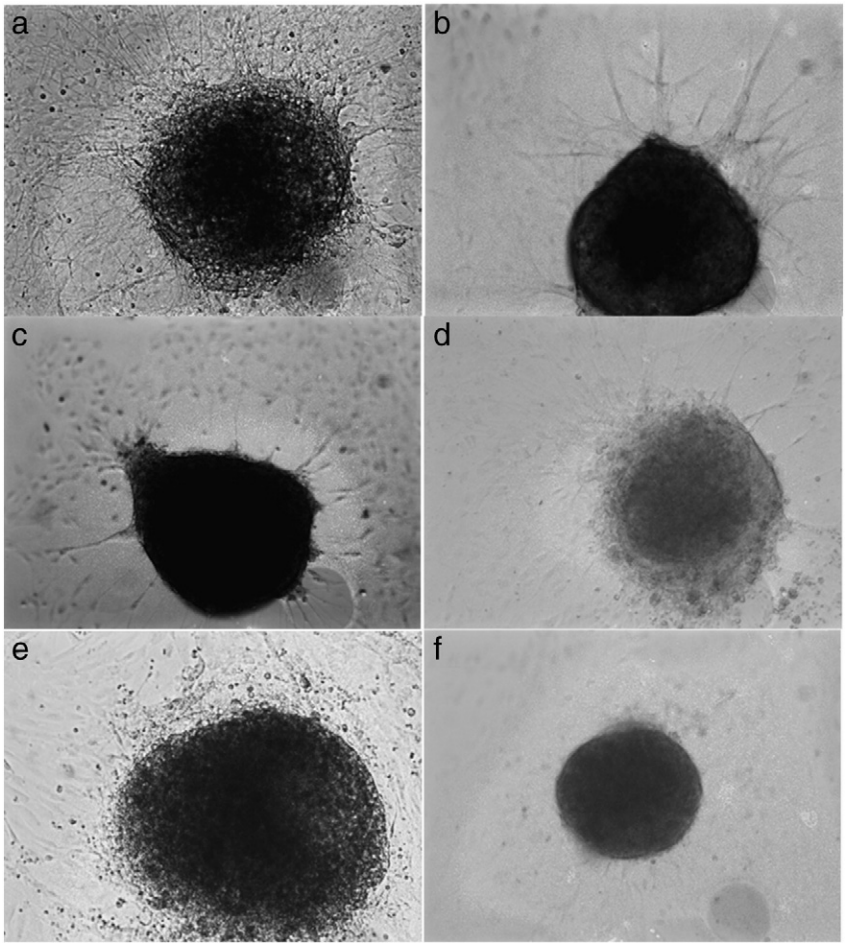


**Fig. 8.** The presence of soluble NT-3 in the cell culture media increases the average number of neurites per ganglion. At 28 d the potency of NT-3 released from the (a) $MgCO_3$ formulation was similar to the (b) 100 ng/mL positive control; (c) no excipient and (d) trehalose/hyaluronan formulations yielded an intermediate number of neurites; and the (e) PEG 400 formulation was similar to the (f) negative control.

through hydrophobic interactions over the span of hours [4], we propose that this association slows protein diffusion through a restrictive membrane-like mechanism, thereby attenuating release [47,48]. This interpretation suggests that an enhanced sustained release profile is possible for a wide range of molecules from composite HAMC relative to freely suspended PLGA particles because the mechanism is independent of the properties of the drug. This view is supported by the report of attenuated release of PLGA-encapsulated dbcAMP (Mw = 0.46 kDa), EGF (Mw = 6.2 kDa), and IgG (Mw = 150 kDa) from composite HAMC [3]. This mechanistic explanation is further strengthened by the identical degradation rate of PLGA whether dispersed in HAMC or not. Importantly, the similar degradation profile elucidated in Fig. 2 for PLGA nanospheres in HAMC *vs.* in buffer, suggests that the environment within PLGA particles in composite HAMC is similar to that of PLGA in suspension. The improved sustained release of α-chymotrypsin from composite HAMC relative to PLGA alone and the conclusion that the particle microenvironment was similar in both cases led us to formulate NT-3 in composite HAMC. Since this system demonstrated the capacity for sustained release, we next sought to assess the stability of NT-3, which is a concern in PLGA particles [22].

We explored strategies to improve the stability of NT-3 during processes associated with nanoparticle fabrication, drug release, and storage. The process of encapsulation in PLGA negatively affects protein stability at multiple points in the synthesis to the extent that only 40% of encapsulated NT-3 was detected in initial particle formulations (Fig. 3a). Testing the effects of sonication and lyophilization on NT-3 in solution failed to isolate the source of bioactivity loss because these operations damaged NT-3 more than encapsulation itself (Fig. 3b,c), indicating that PLGA is an important stabilizer for NT-3. Dissolved PLGA may preserve protein activity by increasing solution viscosity during sonication [38] and providing a hydrogen bonding partner for encapsulated proteins during lyophilization [39].

Considering the NT-3 release profiles (Fig. 6) and the corresponding NT-3 bioactivity data (Fig. 7), it is clear that the nanoparticle formulation with no excipients demonstrated sustained, bioactive release over 28 d, greater than that observed by co-encapsulation with trehalose and hyaluronan. These data suggest that any pores formed by these co-encapsulants are likely too small or too poorly interconnected to increase NT-3 release rate, as has been observed in other systems [43]. ELISA and DRG results indicate that co-encapsulation of PEG 400 reduced the duration of bioactive NT-3 release from 28 d to 14 d, with the bulk of release occurring in the first 7 d. While PEG 400 did not meet our design criteria of prolonged release, co-encapsulation with $MgCO_3$ did, demonstrating improved bioactivity up to 28 d compared to the control. Interestingly, 28 d release profiles using PEG 400 as a co-encapsulant was once previously reported in significantly larger, 30 μm PLGA microspheres for another neurotrophin, NGF [37]. The discrepancy between our data and the previously published data may be explained by the significant difference in particle diameters. Release was extended from the larger 30 μm particles because their surface area to volume ratio is 150 times smaller than the 200 nm particles used in the current work. This smaller ratio slows water uptake, drug diffusion, and matrix degradation.

Co-encapsulation with $MgCO_3$ reduced the released fraction of NT-3 and significantly improved its bioactivity over 28 d relative to all other groups. Magnesium carbonate crystals located near the surface of the PLGA particles likely contribute to the increased burst release of NT-3, as this salt can rapidly dissolve in solution, resulting in pore formation near the surface of the particles. The microenvironment in PLGA particles has been reported to be as low as pH 1.5 to pH 3 due to the acidic oligomers produced by the hydrolytic degradation of ester bonds in PLGA [49], an environment in which NT-3 was shown to be particularly sensitive. The release profile and bioactivity of NT-3 from PLGA nanoparticles co-encapsulated with $MgCO_3$ suggest that $MgCO_3$ neutralizes acidic PLGA degradation products in the same way as has been reported for microspheres [50]. The autocatalytic degradation mechanism of PLGA is slowed, thereby reducing the rate of NT-3 release. Given the susceptibly of NT-3 to low pH, the $MgCO_3$ likely maintains a higher pH within the PLGA nanoparticles than would be expected in PLGA alone.

These results demonstrate that sustained release of bioactive NT-3 can be achieved from the proposed composite HAMC drug delivery system. It was discovered that the methyl cellulose in HAMC adheres to dispersed PLGA particles through hydrophobic interactions, a previously unknown mechanism. This understanding could lead to the sustained delivery of a wide range of hydrophilic molecules from this system without disturbing the degradation kinetics of the PLGA. Co-encapsulation of PEG 400 significantly improved NT-3 detection immediately after encapsulation, highlighting the value of this additive during the processing. Yet, PEG 400 decreased the release duration of NT-3 from 28 d to 7 d, which prevented its addition to other long-term release formulations. The trehalose + hyaluronan formulation was also eliminated from further evaluation because it was outperformed by the excipient-free formulation. Specifically, the excipient-free formulation had similar release kinetics (Fig. 6a) and a higher total release amount (Fig. 6b) and bioactivity (Fig. 7). Co-encapsulated $MgCO_3$ dramatically enhanced the bioactivity of NT-3 up to 28 d, which was attributed to the ability of $MgCO_3$ to neutralize the low pH inside PLGA particles, an environment in which NT-3 was shown to be particularly vulnerable to structural damage. Since the $MgCO_3$ formulation demonstrated measurable release over 28 d and elicited the most neurite outgrowth from DRG, it is the preferred preparation for 28 d delivery. Importantly, the proposed drug delivery system offers a total deliverable NT-3 amount that is comparable to similar systems, including NT-3 delivery from a fibrin gel [51] and from microtubes embedded in an agarose gel [10]. We are encouraged by the previously reported *in vivo* biocompatibility of nanoparticle/HAMC composite drug delivery system [4] in addition to the pharmacologically relevant dose, and the sustained and bioactive release of NT-3 in the $MgCO_3$ formulation. Future studies will assess the efficacy of this formulation *in vivo*.

## Acknowledgments

We are grateful for financial support from the Canadian Institutes of Health Research (MSS) and for fellowship support from both the Ontario Graduate Scholarships in Science and Technology (JCS) and the Natural Sciences and Engineering Research Council of Canada (JCS, MDB). The authors would like to express their gratitude to Dr. Ying Fang Chen for assistance with the dorsal root ganglia bioassay, Dr. Philip Y.K. Choi, University of Alberta for a helpful discussion regarding the mathematical model, Dr. Shawn Owen and Karyn Ho for helpful comments, and Karyn Ho for the graphical abstract.

## Appendix A. Supplementary data

Supplementary data to this article can be found online at doi:10.1016/j.jconrel.2012.03.024.

## References

[1] S. Thuret, L.D.F. Moon, F.H. Gage, Therapeutic interventions after spinal cord injury, Nature 7 (2006) 628–643.
[2] D. Aprili, O. Bandschapp, C. Rochlitz, A. Urwyler, W. Ruppen, Serious complications associated with external intrathecal catheters used in cancer pain patients: a systematic review and meta-analysis, Anesthesiology 111 (2009) 1346–1355.
[3] M.D. Baumann, C.E. Kang, J.C. Stanwick, Y. Wang, H. Kim, Y. Lapitsky, M.S. Shoichet, An injectable drug delivery platform for sustained combination therapy, J. Controlled Release 138 (2009) 205–213.
[4] M.D. Baumann, C.E. Kang, C.H. Tator, M.S. Shoichet, Intrathecal delivery of a polymeric nanocomposite hydrogel after spinal cord injury, Biomaterials 31 (2010) 7631–7639.
[5] C.E. Kang, P.C. Poon, C.H. Tator, M.S. Shoichet, A new paradigm for local and sustained release of therapeutic molecules to the injured spinal cord for neuroprotection and tissue repair, Tissue Eng. Part A 15 (2009) 595–604.

[6] D. Gupta, C.H. Tator, M.S. Shoichet, Fast-gelling injectable blend of hyaluronan and methylcellulose for intrathecal, localized delivery to the injured spinal cord, Biomaterials 27 (2006) 2370–2379.
[7] L.F. Reichardt, Neurotrophin-regulated signalling pathways, Philos. Trans. R. Soc. 361 (2006) 1545–1564.
[8] R.C. Robinson, C. Radziejewski, G. Spragon, J. Greenwald, M.R. Kostura, L.D. Burtnick, D.I. Stuart, S. Choe, E.Y. Jones, The structures of the neurotrophin 4 homodimer and the brain-derived neurotrophic factor/neurotrophin 4 heterodimer reveal a common Trk-binding site, Protein Sci. 8 (1999) 2589–2597.
[9] S.J. Taylor, S.E. Sakiyama-Elbert, Effect of controlled delivery of neurotrophin-3 from fibrin on spinal cord injury in a long term model, J. Controlled Release 116 (2006) 204–210.
[10] H. Lee, R.J. McKeon, R.V. Bellamkonda, Sustained delivery of thermostabilized chABC enhances axonal sprouting and functional recovery after spinal cord injury, PNAS 107 (2010) 3340–3345.
[11] M. Yu-Hai, Y. Zhang, L. Cao, J.-C. Su, Z.-W. Wang, A.-B. Xu, S.-C. Zhang, Effect of neurotrophin-3 genetically modified olfactory ensheathing cells transplantation on spinal cord injury, Cell Transplant. 19 (2010) 167–177.
[12] N. Comolli, B. Neuhuber, I. Fischer, A. Lowman, In vitro analysis of PNIPAAm-PEG, a novel, injectable scaffold for spinal cord repair, Acta Biomater. 5 (2009) 1046–1055.
[13] J.A. Burdick, M. Ward, E. Liang, M.J. Young, R. Langer, Stimulation of neurite outgrowth by neurotrophins delivered from degradable hydrogels, Biomaterials 27 (2006) 452–459.
[14] J.H. Brock, E.S. Rosenzweig, R. Moseanko, L.A. Havton, V.R. Edgerton, M.H. Tuszynski, Local and remote growth factor effects after primate spinal cord injury, J. Neurosci. 30 (2010) 9728–9737.
[15] P. Lu, H. Yang, L.L. Jones, M.T. Filbin, M.H. Tuszynski, Combinatorial therapy with neurotrophins and cAMP promotes axonal regeneration beyond sites of spinal cord injury, J. Neurosci. 24 (2004) 6402–6409.
[16] J.V. Coumans, T.T.S. Lin, H.N. Dai, L. MacArthur, M. McAtee, C. Nash, B.S. Bregman, Axonal regeneration and functional recovery after complete spinal cord transection in rats by delayed treatment with transplants and neurotrophins, J. Neurosci. 21 (2001) 9334–9344.
[17] M.H. Tuszynski, Cellular delivery of neurotrophin-3 promotes corticospinal axonal growth and partial functional recovery after spinal cord injury, J. Neurosci. 17 (1997) 5560–5572.
[18] T. Peternel, R. Komel, Isolation of biologically active nanomaterial (inclusion bodies) from bacterial cells, Microb. Cell Fact. 9 (2010).
[19] W. Wang, Lyophilization and development of solid protein pharmaceuticals, Int. J. Pharm. 203 (2000) 1–60.
[20] A. Hawe, J.C. Kasper, W. Friess, W. Jiskoot, Structural properties of monoclonal antibody aggregates induced by freeze–thawing and thermal stress, Eur. J. Pharm. Sci. 38 (2009) 79–87.
[21] M.A. Ibrahim, A. Ismail, M.I. Fetouh, A. Gopferich, Stability of insulin during the erosion of poly (lactic acid) and poly (lactic-co-glycoilic acid) microspheres, J. Controlled Release 106 (2005) 241–252.
[22] U. Bilati, E. Allemann, E. Doelker, Strategic approaches for overcoming peptide and protein instability within biodegradable nano- and microparticles, Eur. J. Pharm. Sci. 59 (2005) 375–388.
[23] E.S. Lee, M.J. Kwon, H. Lee, J.J. Kim, Stabilization of protein encapsulated in poly (lactide-co-glycolide) microspheres by novel viscous S/W/O/W method, Int. J. Pharm. 331 (2007) 27–37.
[24] M.L. Houchin, E.M. Topp, Chemical degradation of peptides and proteins in PLGA: a review of reactions and mechanisms, J. Pharm. Sci. 97 (2008) 2395–2404.
[25] X. Wen, P.A. Tresco, Fabrication and characterization of permeable degradable poly (DL-lactide-co-glycolide) (PLGA) hollow fiber phase inversion membranes for use as nerve tract guidance channels, Biomaterials 27 (2006) 3800–3809.
[26] Y. Yeo, K. Park, Control of encapsulation efficiency and initial burst in polymeric microparticle systems, Arch. Pharmacol. Res. 27 (2004) 1–12.
[27] M.C. Jimenez Hamann, E.C. Tsai, C.H. Tator, M.S. Shoichet, Novel intrathecal delivery system for treatment of spinal cord injury, Exp. Neurol. 182 (2003) 300–309.
[28] N. Faisant, J. Siepmann, J.P. Benoit, PLGA-based microparticles: elucidation of mechanisms and a new, simple mathematical model quantifying drug release, Eur. J. Pharm. Sci. 15 (2002) 355–366.
[29] C. Raman, C. Berkland, K. Kim, D.W. Pack, Modeling small-molecule release from PLG microspheres: effects of polymer degradation and nonuniform drug distribution, J. Controlled Release 103 (2005) 149–158.
[30] M.D. Baumann, C.E. Kang, J.C. Stanwick, Y. Wang, H. Kim, Y. Lapitsky, M.S. Shoichet, An injectable drug delivery platform for sustained combination therapy, J. Control. Release 138 (2009) 205–213.
[31] A. Hurtado, L.D.F. Moon, V. Maquet, B. Blits, R. Jerome, M. Oudega, Poly(D, L-lactic acid) macroporous guidance scaffolds seeded with Schwann cells genetically modified to secrete a bi-functional neurotrophin implanted in the completely transected adult rat thoracic spinal cord, Biomaterials 27 (2006) 430–442.
[32] B. Blits, P.A. Dijkhuizen, G.J. Boer, J. Verhaagen, Intercostal nerve implants transduced with an adenoviral vector encoding neurotrophin-3 promote regrowth of injured rat corticospinal tract fibers and improve hindlimb function, Exp. Neurol. 164 (2000) 25–37.
[33] C.P. Riley, T.C. Cope, C.R. Buck, CNS neurotrophins are biologically active and expressed by multiple cell types, J. Mol. Histol. 35 (2004) 771–783.
[34] M. Kose, J. Hasenwinkel, P.A. Rice, Drug release properties of the enzyme chondroitinase (cABC) from PLGA nanospheres into the spinal cord injury area, Al ChE Annual Meeting, Conference Proceedings, 2007.
[35] L.K. Chiu, W.J. Chiu, Y.-L. Cheng, Effects of polymer degradation on drug release - a mechanistic study of morphology and transport properties in 50:50 poly (DL-lactide-co-glycolide), Int. J. Pharm. 126 (1995) 169–178.
[36] L. Li, S.P. Schwendeman, Mapping neutral microclimate pH in PLGA microspheres, J. Controlled Release 101 (2005) 163–173.
[37] J.-M. Pean, F. Boury, M.-C. Venier-Julienne, P. Menei, J.-E. Proust, J.-P. Benoit, Why does PEG 400 co-encapsulation improve NGF stability and release from PLGA biodegradable microspheres? Pharm. Res. 16 (1999) 1294–1299.
[38] L.B. Feril Jr., T. Kondo, Major factors involved in the inhibition of ultrasound-induced free radical production and cell killing by pre-sonication incubation or by high cell density, Ultrason. Sonochem. 12 (2005) 353–357.
[39] J.F. Carpenter, J.H. Crowe, T. Arakawa, Comparison of solute-induced protein stabilization in aqueous solution and in frozen and dried state, J. Dairy Sci. 73 (1990) 3627–3636.
[40] M. Rabe, D. Verdes, S. Seeger, Understanding protein adsorption phenomena at solid surfaces, Adv. Colloid Interface Sci. 162 (2011) 87–106.
[41] M. Bhattacharya, N. Jain, S. Mukhopadhyay, Insights into the mechanism of aggregation and fibril formation from bovine serum albumin, J. Phys. Chem. B 115 (2011) 4195–4205.
[42] S.T. Kelly, A.L. Zydney, Effects of intermolecular thiol–disulfide interchange reactions on BSA fouling during microfiltration, Biotechnol. Bioeng. 44 (1994) 972–982.
[43] R. Dorati, C. Colonna, I. Genta, T. Modena, B. Conti, Effect of porogen on the physico-chemical properties and degradation performance of PLGA scaffolds, Polym. Degrad. Stabil. 95 (2010) 694–701.
[44] S.J. Taylor, J.W. McDonald, S.E. Sakiyama-Elbert, Controlled release of neurotrophin-3 from fibrin gels for spinal cord injury, J. Controlled Release 98 (2004) 281–294.
[45] A. Giteau, M.C. Venier-Julienne, A. Aubert-Pouessel, J.P. Benoit, How to achieve sustained and complete protein release from PLGA-based microparticles, Int. J. Pharm. 350 (2008) 14–26.
[46] N. Schupper, Y. Rabin, M. Rosenbluh, Multiple stages in the aging of a physical polymer gel, Macromolecules 41 (2008) 3983–3994.
[47] P. Arora, P.N. Tandon, Mathematical models for drug delivery to chronic patients, Appl. Math. Model. 33 (2009) 692–705.
[48] B.-H. Chen, D.J. Lee, Slow release of drug through deformed coating film: effects of morphology and drug diffusivity in the coating film, J. Pharm. Sci. 90 (2001) 1478–1496.
[49] K. Fu, D.W. Pack, A.M. Klibanov, R. Langer, Visual evidence of acidic environment within degrading poly (lactic-co-glycolic acid) (PLGA) microspheres, Pharm. Res. 17 (2000) 100–107.
[50] G. Zhu, S.R. Mallery, S.P. Schwendeman, Stabilization of proteins encapsulated in injectable poly (lactide-co-glycolide), Nat. Biotechnol. 18 (2000) 52–57.
[51] S.J. Taylor, E.S. Rosenzweig, J.W. McDonald III, S.E. Sakiyama-Elbert, Delivery of neurotrophin-3 from fibrin enhances neuronal fiber sprouting after spinal cord injury, J. Controlled Release 113 (2006) 226–235.